UPDATING DIGITAL GEOGRAPHIC DATABASE USING VEHICLE-BORNE LASER SCANNERS AND LINE CAMERAS

Huijing Zhao, Ryosuke Shibasaki

Center for Spatial Information Science, Univ. of Toky
{chou, shiba}@skl.iis.u-tokyo.ac.jp

Commission III, WG 6

KEY WORDS: Data Fusion, Vehicle-borne, Laser Range Scanner, Urban 3D

ABSTRACT:

VLMS is a mobile mapping system, where three single-row laser range scanners, six line CCD cameras as well as a GPS/INS based navigation unit are mounted on a van, measuring object geometry as well as texture along the street. This paper contributes to a method of fusing the data output of VLMS with existing geographic data sources, where focus is cast on the rectification of GPS/INS parameters, which might be quite erroneous in urban area. An algorithm is developed to correct four parameters of each GPS/INS update, i.e. xyz coordinates of vehicle position and yaw angle of vehicle orientation, by registering the laser points of VLMS with an existing data source, e.g. DSM. The algorithm is examined using the VLMS data that are taken in GINZA area, Tokyo. Manually assigning 18 sets of tie-points, GPS/INS parameters are corrected automatically and efficiently, so that the laser points of VLMS are matched to a DSM. In data fusion, a set of objects are extracted from the rectified VLMS data using an interface that was developed in our previous research, which contains of commercial sign board, traffic sign/signal, road boundary, road lights and so on. They are integrated with a 1:2500 3D map that consists of building frames only. In addition, line images of VLMS are projected onto the building facades of the 3D map, and textures are generated in an automated way.

1. INTRODUCTION

Up to now, many research efforts in photogrammetry and remote sensing community have been devoted to the study of aerial or satellite based mapping technologies for the reconstruction of 3D urban objects (e.g. Collins 1994, Gruen 1998), and a vast amount of geographic database has been established. Normally, aerial or satellite based survey can cover relatively wide area, but fail in capturing urban details due to the limitation of spatial resolution and viewing angle. On the other hand, mobile mapping system (MMS) has emerged recently as a promising survey technique for collecting detailed spatial data from the ground. With the development of automobile navigation system, 3D GIS (*Geographic Information System*), ITS (*Intelligent Transportation System*), and applications using virtual and augmented reality, 3D urban database containing the details, such as sidewall (facade) of buildings, traffic sign/signal, commercial signboards etc., are found of increasing importance. A number of mobile mapping systems have been developed (e.g. Ellum and El-Sheimy 2000, He and Orvets 2000, Silva et.al.2000). A comprehensive examination of MMS can be found in Li 1997 or El-Sheimy 1999. The mapping technologies from either air or ground have their advantages and drawbacks. It is demonstrated that MMS has efficiency in generating detailed spatial database. Whereas, it lacks spatial coverage, which can be compensated using other traditional survey techniques taking data from the air or satellite. It is important that the data sources collected using both technologies are fused, so that a more comprehensive geographic database can be generated.

A mobile mapping system called VLMS (*Vehicle-borne Laser Measurement System*) has been developed in a joint research effort between Asia Air Survey Co. Ltd and ours, aiming at collecting the detailed spatial data in central urban area. Except the GPS (*Global Positioning System*)/INS (*Inertial Navigation System*) based navigation unit, three single-row laser range scanners (briefly called "laser scanner") and six line CCD cameras (briefly called "line camera") are mounted on a van, mapping object's geometry as well as texture along streets. A framework for automatically reconstructing textured 3D models of buildings, roads and trees using vehicle-borne laser range and line images (Zhao and Shibasaki 2003a), and an interface for extracting a broad range of urban objects, such as commercial signboard, road boundary, traffic sign/signal, telegram pole/cable and so on, in a semi-automatic manner (Zhao and Shibasaki, 2003b) were developed. Efficiency of the system for generating a database of urban details was demonstrated through a number of real experiments in central Tokyo. However, since both laser range and line images are geo-referenced directly using the position and orientation parameters from GPS/INS based navigation unit, the geo-referenced data sets as well as the modeling results might be quite erroneous especially in central town, and have to be rectified before being exploited to update existing geographic database.

In the GPS/INS based navigation unit, GPS measures vehicle's position using satellite signals, which might be heavily obstructed by bridges, trees, tunnels and buildings in urban area. INS, consisting of accelerometers and gyroscopes, measures the velocity and direction changes of the vehicle with high accuracy for only short periods. Accelerometer biases and gyro drifts grow rapidly with time. The GPS/INS combination takes advantages of each other. Velocity and direction changes from INS output are exploited to interpolate vehicle positions during the period of GPS signal outage, while GPS measurements are utilized to reset and update INS system. However, accuracy and reliability of GPS/INS based direct geo-referencing is degraded when GPS signals are blocked for a long period. The direct geo-referencing using GPS/INS combination performs poor in downtown area. When overlapping the data outputs of VLMS

that are taken in central Tokyo, such as GINZA area, with other existing geographic data, such as DSM (*Digital Surface Model*) or digital map, disagreement between different data sets is found (see Figure 8 for an example), and it varies along the vehicle's measurement course as the accuracy of GPS/INS combination changes with the local surroundings.

This paper contributes to a method of fusing the data output of VLMS with existing geographic database. An algorithm is developed to correct the position and orientation parameters at each GPS/INS update using e.g. a DSM as the ground truth. Rectification is conducted in two subsequent steps, horizontal and vertical registration. First, a number of tie-points are assigned manually establishing correspondences between the building frames that are measured by the geo-referenced laser range data (called laser points) of VLMS and those in DSM. Three parameters at each GPS/INS update, i.e. (x,y) coordinates of vehicle position and yaw angle (κ) of vehicle orientation, are corrected to fit VLMS data to the ground truth. Secondly, a vertical registration is conducted to match the ground elevations along vehicle's measurement course, where z coordinate of vehicle position at each GPS/INS update is adjusted. The algorithm is tested using the VLMS data of GINZA area, one of the major commercial centers in Tokyo. Vehicle's measurement course lasted for about 15.7km. A DSM, which was generated from an air-borne laser data that has a ground resolution of 1 m^2 and a ground coverage of about 15.9 km^2, is used to rectify the GPS/INS parameters of VLMS data. In data fusion, a set of objects are extracted from the rectified VLMS data, consisting of commercial signboard, traffic sign/signal, road light, road boundary and so on. They are integrated with a 1:2500 3D map that has building frame only. In addition, line images of VLMS are projected onto the building facades of the 3D map to generate textures automatically. In the followings, we will first briefly introduce the sensor system of VLMS as well as the method for geo-referencing laser range and line images. The algorithm for rectifying GPS/INS parameters is presented next. Experimental results as well as the applications of data fusing in updating an existing map are addressed subsequently. In this paper, homogenous notations are exploited to address all the transformation matrixes.

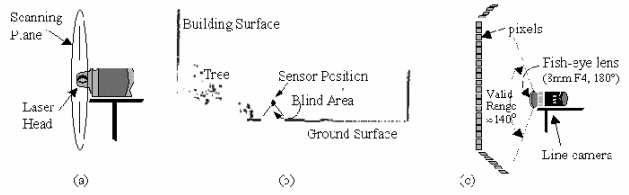

Figure 1. Laser range finder (LD-A) and line camera (a) configuration of LD-A, (b) range points in a scan line, (c) configuration of line camera.

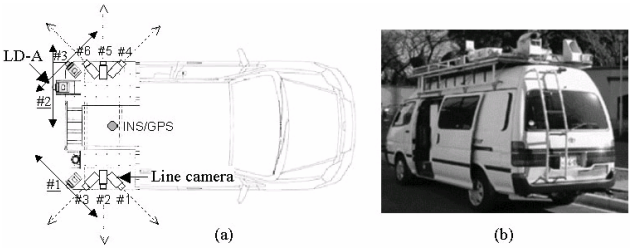

Figure 2. Conceptual figures of Geo-referencing data sources (a) geo-referencing of range scan line, (b) geo-referencing of line image.

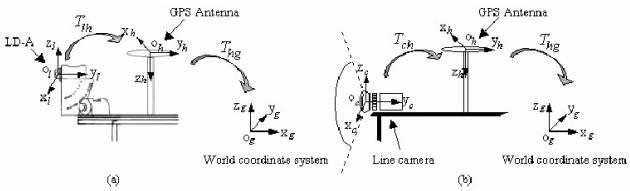

Figure 3. Conceptual figures of Geo-referencing data sources (a) geo-referencing of range scan line, (b) geo-referencing of line image.

2. SENSOR SYSTEM AND DATA OUTPUTS OF VLMS

2.1 Sensor system

VLMS consists of three different kinds of sensors and each for a specific purpose. They are laser range scanners - the sensor for measuring object geometry, line cameras - the sensor for capturing object texture, and GeoMaster - the moving platform with a GPS/INS based navigation unit.

Single-row laser range scanners, LD-A, produced by IBEO Lasertechnik, are exploited in the sensor system (see Figure 1(a)). In one scanning (a range scan line), LD-A profiles 480 range points of the surroundings on the scanning plane within 300 degrees. A blind area of 60 degree exists due to the hardware configuration (see Figure 1(b)). LD-A has a maximum range distance of 100 meter and an average error of 3cm. Frequency of LD-A is 20Hz, implying that it profiles 20 range scan lines per second.

Line CCD cameras are implemented in the sensor system. Each has a 8mm F4 fish-eye lens with a vision field of 180 degree on it (see Figure 1(c)). In each snapshot, a single-row image (line image) of 1*2048 pixels is captured on the scanning plane. Among the 2048 pixels, about 224 pixels (¡Ö20^o) on each side are discarded due to high lens distortion. Line images are captured at a rate of 80Hz by each line camera.

The measurement vehicle (Figure 2(b)) - GeoMaster is equipped with a high accurate GPS/INS based navigation system - HISS (Konno et al. 2000). Three LD-As and six line cameras are mounted on the roof of GeoMaster as shown in Figure 2(a). Both LD-As and line cameras are installed with their scanning planes at different angles to reduce occlusion from e.g. trees. In this research, all exterior calibration parameters (relative angles and distances) between sensor's local coordinate systems are obtained through physical measurement; all interior calibration parameters (e.g. focus length) are obtained from maker or sensor's specifications. For data measurement, all sensors keep recording data sources as the vehicle moves ahead. When GeoMaster moves at a speed of 20km/h, line images are captured at an interval of about 6.9cm by each line camera, range scan lines are profiled at an interval of about 27.8cm by each LD-A, locations and directions of the vehicle are measured by GPS/INS at an interval of about 20cm. GPS/INS parameters are linearly interpolated and associated to each range scan line and line image.

2.2 Geo-referencing data sources

Figure 3 shows the conceptual figures of geo-referencing range scan lines and line images to a world coordinate system. According to the GPS/INS parameters that are associated to each range scan line and line image, a transformation matrix

T_{hg} from the coordinate system of HISS to a world coordinate system is calculated, where the origin of HISS is at the center of GPS antenna. On the other hand, a transformation matrix T_{lh} from the coordinate system of LD-A and a transformation matrix T_{ch} from the coordinate system of line camera to the coordinate system of HISS are calculated based on the exterior calibration parameters. A laser point with a range distance of *r* at the angle of α on scanning plan is geo-referenced to the world coordinate system as follow,

$$(x, y, z, 1)^T = T_{hg} T_{lh} (-r \sin\alpha, 0, -r \cos\alpha, 1)^T \quad (1)$$

In the case of line image, focus length (*f*) of the line camera as well as a formula defining the relationship between the index of an image pixel (*h*) and its projection angle (ω) towards the projection axis is obtained from sensor's specification.

$$\omega = 2 \times \arcsin((h - o)/2/f) \quad (2)$$

where *o* is the image center, which is obtained by doing physical measurement using sample images. Using formula 2, projection vector of the image pixel (*h*) is geo-referenced to the world coordinate system as follows,

$$(x, y, z, 0)^T = T_{hg} T_{ch} (0, -\cos\omega, \sin\omega, 0)^T \quad (3)$$

An example of line images, a view of geo-referenced laser points, as well as a projection of laser points onto line images is shown in Figure 4.

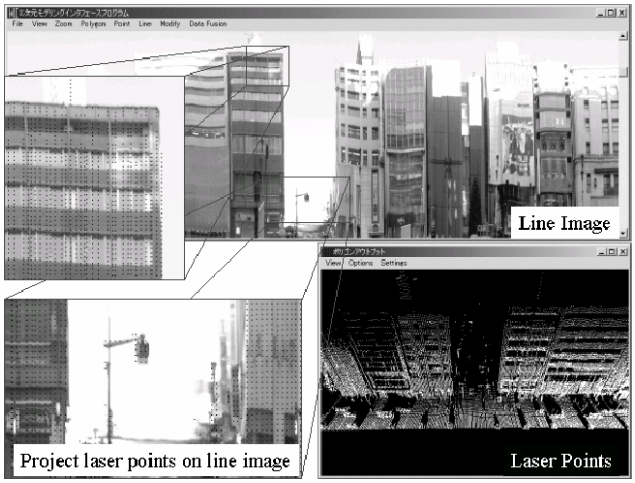

Figure 4. An example of the geo-referenced laser points and line images

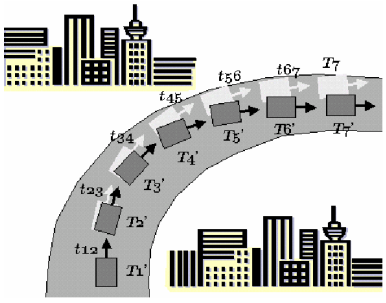

Figure 5. A motivational example of erroneous geo-referencing

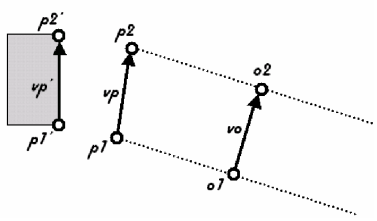

Figure 6. A set of tie points on building corners

3. RECTIFICATION OF GPS/INS PARAMETERS

In the followings, we will first introduce the method for rectifying GPS/INS parameters at each updates using a number of ground truths. The method for obtaining the true value of position and orientation parameters at a number of GPS/INS updates is addressed subsequently.

3.1 Rectification using a number of ground truths

Let (o_x, o_y, o_z) denote the xyz coordinates of vehicle position, (ω, ψ, κ) denote the roll, pitch and yaw angles of vehicle orientation, transformation from HISS to the world coordinate system can be formulated as follows.

$$T_{hg} = Shv \cdot R_\kappa \cdot R_\psi \cdot R_\omega \quad (4)$$

where

$$Shv = \begin{pmatrix} 1 & 0 & 0 & o_x \\ 0 & 1 & 0 & o_y \\ 0 & 0 & 1 & o_z \\ 0 & 0 & 0 & 1 \end{pmatrix}, \quad R_\kappa = \begin{pmatrix} \cos\kappa & -\sin\kappa & 0 & 0 \\ \sin\kappa & \cos\kappa & 0 & 0 \\ 0 & 0 & 1 & 0 \\ 0 & 0 & 0 & 1 \end{pmatrix},$$

$$R_\psi = \begin{pmatrix} \cos\psi & 0 & -\sin\psi & 0 \\ 0 & 1 & 0 & 0 \\ \sin\psi & 0 & \cos\psi & 0 \\ 0 & 0 & 0 & 1 \end{pmatrix}, \quad R_\omega = \begin{pmatrix} 1 & 0 & 0 & 0 \\ 0 & \cos\omega & -\sin\omega & 0 \\ 0 & \sin\omega & \cos\omega & 0 \\ 0 & 0 & 0 & 1 \end{pmatrix}.$$

In this research, four parameters at each GPS/INS update, i.e. o_x, o_y, o_z of vehicle position andκ of vehicle orientation, are corrected, while pitch and roll angles remain as they are, as the errors inside are not so obvious comparing to other parameters. Let

$$\tilde{p} = (\tilde{x}, \tilde{y}, \tilde{z}, 1)^T = R_\psi R_\omega T_{lh} (-r \sin\alpha, 0, -r \cos\alpha, 1)^T \quad (5)$$

denote the calculations on the parameters that will not be adjusted. Geo-referencing of a laser point $p = (x, y, z, 1)^T$ can be re-formularized as follows,

$$p = Shv \cdot R_\kappa \cdot \tilde{p} \quad (6)$$

More specifically,

$$\begin{aligned} p_x &= \tilde{p}_x * \cos\kappa - \tilde{p}_y * \sin\kappa + o_x \\ p_y &= \tilde{p}_x * \sin\kappa + \tilde{p}_y * \cos\kappa + o_y \\ p_z &= \tilde{p}_z + o_z \end{aligned} \quad (7)$$

Figure 5 shows a motivational example of erroneous geo-referencing, where the denotation of T_{hg}^i is simplified to T_i, representing the transformation matrix that is composed of the position and orientation parameters at GPS/INS update *#i*. T_i' denotes the true value of T_i, $t_{ij} = T_i^{-1} \cdot T_j$ is the vehicle's relative motion (relative transformation) from GPS/INS update *#i* to *#j*. Suppose the true transformation matrixes at the GPS/INS updates *#s* and *#e* are known, where $T_s' = T_s$, $T_e' \neq T_e$,

and $s<e$, the relative transformations $t_{i,i+1}$, $s<i<e$ between each pair of successive GPS/INS updates are adjusted to achieve global matching between T_e and T_e', while maintaining local consistencies.

Relative transformations $t_{i,i+1}$, $s<i<e$ are adjusted in an iterative way, where in the kth iteration, a $\Delta t^k_{i,i+1}$ is calculated for each $t^k_{i,i+1}$, $s<i<e$. $t^k_{i,i+1}$ is updated as follows.

$$\Delta t^k_{i,i+1} = \frac{1}{e-s} \cdot t^k_{i+1,i+2}{}^{-1} \cdots t^k_{e-1,e}{}^{-1} \cdot T_e' \cdot T_s^{-1} \cdot t^k_{s,s+1}{}^{-1} \cdots t^k_{i-1,i}{}^{-1} \tag{8}$$

$$t^{k+1}_{i,i+1} = \Delta t^k_{i,i+1} \cdot t^k_{i,i+1} \tag{9}$$

The process continued until $\left\| T_e^{-1} \cdot T_e' \right\|$ is smaller than a given threshold or can never be minimized any more, where $\| \cdot \|$ is the norm of the vector. Denote $\bar{t}_{i,i+1}$ and $\bar{T}_j$ as the rectified $t_{i,i+1}$ and T_j respectively. $\bar{T}_j$, $s < j \le e$ are obtained by sequentially aligning $\bar{t}_{i,i+1}$s as follows.

$$\begin{aligned} \bar{T}_j &= \bar{T}_{j\text{-}1} \cdot \bar{t}_{j\text{-}1,j} \\ &= \bar{T}_s \cdot \bar{t}_{s,s+1} \cdots \bar{t}_{i,i+1} \cdots \bar{t}_{j\text{-}1,j} \end{aligned} \tag{9}$$

Since GPS/INS parameters drift in a non-linear way according to the local surroundings, they are rectified using the ground truths at a number of updates. Let T_{g1}', T_{g2}',…,T_{gn}' represents the n true transformations at the GPS/INS updates *#g1, #g2, …, #gn*, where *g1<g2<…<gn*. Correction of T_is at all GPS/INS updates is conducted as follows.

Algorithm Rectification of GPS/INS parameters using a number of ground truths
Input GPS/INS measured transformations $\{T_i \mid 1 \le i \le N\}$
Input n ground truths $\{T_{gk}' \mid 1 \le g_1 \le g_k \le g_n \le N\}$
Output Rectified transformations $\{\bar{T}_i \mid 1 \le i \le N\}$

for *k=1:n*
  if *k=1*
    let $\Delta T = T_{g1}^{-1} \cdot T_{g1}'$
    for *i=1:N* $\{\bar{T}_i = T_i \cdot \Delta T\}$
  else
    calculate $\{\bar{t}_{i,i+1} \mid g_{k-1} \le i \le g_k - 1\}$
    for *i=* $g_{k-1} : g_k - 1$ $\{T_i = T_{i-1} \cdot \bar{t}_{i-1,i}\}$
    let $\Delta T = T_{gk}^{-1} \cdot T_{gk}'$
    for *i=* $g_k : N$ $\{\bar{T}_i = T_i \cdot \Delta T\}$

3.2 Obtaining the ground truths

In this research, the true transformations at a number of GPS/INS updates are obtained in two levels, so that GPS/INS parameters are rectified in two subsequent steps, horizontal and vertical registration. True values of the horizontal parameters, i.e. o_x, o_y and κ, are obtained using a number of manually assigned tie-points, which reflect the correspondences between the laser points of VLMS and a DSM that is treated as the ground truth. On the other hand, true values of the vertical parameter, i.e. o_z, are obtained by horizontally registering the laser points of VLMS to the data source of ground truth, and sampling the elevation values of the data of ground truth along the vehicle's measurement course.

Obtaining the true values of horizontal parameters: A set of tie points consists of two pairs of closely located corresponding points. Figure 6 shows an example, where p_1 and p_2 are VLMS measurements to building corners from the vehicle positions o_1 and o_2, respectively. p_1' and p_2' corresponds to p_1 and p_2, which are represented by a DSM. Let $(o_{xi}, o_{yi}, \kappa_i)$ denote the horizontal position and orientation parameters obtained from GPS/INS combination at o_i, and $(o_{xi}', o_{yi}', \kappa_i')$ denote their true values. Suppose o_1 and o_2 are near to each other, so that the difference of GPS/INS drifts $(\Delta x, \Delta y, \Delta\kappa)$ between them are ignored. Let $o_{xi}' = o_{xi} + \Delta x$, $o_{yi}' = o_{yi} + \Delta y$, $\kappa_i' = \kappa_i + \Delta\kappa$, $(\Delta x, \Delta y, \Delta\kappa)$ are obtained by matching p_1, p_2 to p_1', p_2' as follows, where p_2 and p_2' serve as the directional points in finding the orientation drift of $\Delta\kappa$, p_1 and p_1' are the axis points, the resulted $\Delta x, \Delta y, \Delta\kappa$ are treated as the GPS/INS drift at o_1.

Considering the horizontal parameters of Formula 7, p_i and p_i', *i=1,2* are represented as follows.

$$p_i = \begin{pmatrix} \cos\kappa_i & -\sin\kappa_i \\ \sin\kappa_i & \cos\kappa_i \end{pmatrix} \cdot \tilde{p} + o_i \tag{11}$$

$$p_i' = \begin{pmatrix} \cos\kappa_i + \Delta\kappa & -\sin\kappa_i + \Delta\kappa \\ \sin\kappa_i + \Delta\kappa & \cos\kappa_i + \Delta\kappa \end{pmatrix} \cdot \tilde{p} + o_i + \begin{pmatrix} \Delta x \\ \Delta y \end{pmatrix} \tag{12}$$

Let $v_p = p_2 - p_1$, $v_p' = p_2' - p_1'$, and $v_o = o_2 - o_1$, it has

$$v_p = \begin{pmatrix} \cos\kappa_2 & -\cos\kappa_1 \\ \sin\kappa_2 & -\sin\kappa_1 \end{pmatrix} \begin{pmatrix} \tilde{p}_{x2} \\ \tilde{p}_{x1} \end{pmatrix} + \begin{pmatrix} -\sin\kappa_2 & \sin\kappa_1 \\ \cos\kappa_2 & -\cos\kappa_1 \end{pmatrix} \begin{pmatrix} \tilde{p}_{y2} \\ \tilde{p}_{y1} \end{pmatrix} + v_o \tag{13}$$

$$v_p' - v_o = \begin{pmatrix} \cos\Delta\kappa & -\sin\Delta\kappa \\ \sin\Delta\kappa & \cos\Delta\kappa \end{pmatrix} (v_p - v_o) \tag{14}$$

Thus $\Delta x, \Delta y, \Delta\kappa$ are obtained as follows.

$$\Delta\kappa = \cos^{-1}\left[(|v_p'| - v_o|) \cdot (|v_p - v_o|) \right] \tag{15}$$

$$\Delta x = p'_{x1} - o_{x1} - \tilde{p}_{x1} * \cos(\kappa_1 + \Delta\kappa) + \tilde{p}_{y1} * \sin(\kappa_1 + \Delta\kappa) \tag{16}$$

$$\Delta y = p'_{y1} - o_{y1} - \tilde{p}_{x1} * \sin(\kappa_1 + \Delta\kappa) - \tilde{p}_{y1} * \cos(\kappa_1 + \Delta\kappa) \tag{17}$$

Where, $|v|$ denotes the normalized vector of v.

Obtaining the true value of vertical parameter: Vertical registration is conducted, after the position and orientation parameters of GPS/INS updates are horizontally rectified, and the laser points of VLMS are horizontally registered to the DSM. GPS/INS updates of VLMS are equally sampled, and at each sampled vehicle position, the ground truth is calculated as follows. Let (o_x, o_y, o_z) be the vehicle position of GPS/INS measurement, $\tilde{o}_z'$ be the elevation value at (o_x, o_y) obtained from the DSM, h is the height from the origin of HISS coordinate system to the ground surface, which is measured previously in calibration process, $o_z' = \tilde{o}_z' + h$ is treated as the true value of o_z at (o_x, o_y).

4. EXPERIMENTAL RESULTS AND APPLICATIONS IN DATA FUSION

A VLMS data that is taken in GINZA area, one of the major commercial centers in Tokyo, lasted for about 15.7km. Figure 7 shows vehicle's measurement course using the building facades that are represented by the laser points of VLMS. See Figure 12 for a strip of the line images and a perspective and close view of the laser points. A DSM, which was generated from an air-borne laser data that has a ground resolution of $1\,m^2$ and a ground coverage of about $15.9\,km^2$, is used to rectify the GPS/INS parameters at each update. In addition, a 1:2500 digital map containing the data of 3D building frames only, where 2D building frames were generated from aerial photos, elevation data for each facade was extracted from an air-borne laser data, are exploited to test the performance in data fusion.

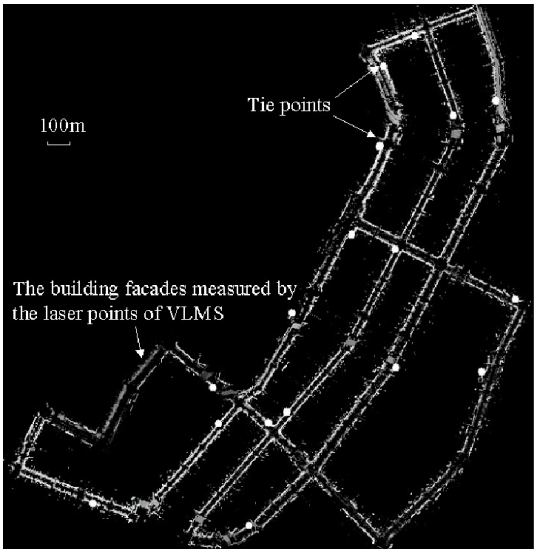

Figure 7. The laser points of VLMS at GINZA area and the distribution of tie-points for horizontal registration

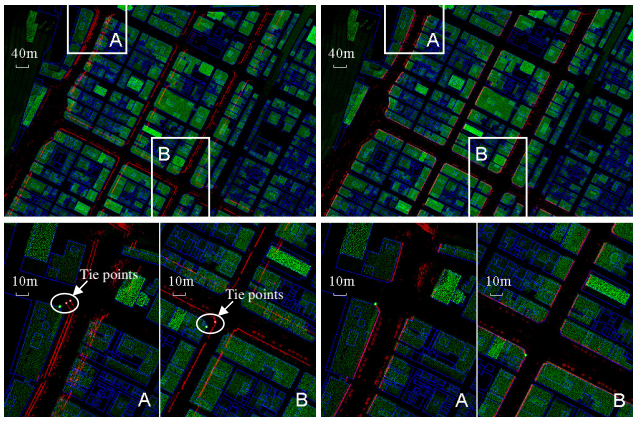

(a) (b)

Figure 8. A result of registering the laser points of VLMS with a DSM

4.1 Experimental results of rectifying VLMS data

Figure 8 shows an overlapping of the three different data sources, where large displacements are found from the laser points of VLMS to other data sets. In the area "A" of Figure 8, vehicle ran along the street a second time after a several ten minutes. Errors in GPS/INS parameters are accumulated much more during this period, so that laser range measurements to the same building facades do not match well, and both drift away from the data of DSM in different patterns. In horizontal registration, 18 sets of tie-points are manually assigned, binding the corresponding building corners that are measured by the laser points of VLMS and the DSM. Distribution of the 18 sets of tie-points is shown in Figure 7. Horizontal parameters at more than 46000 GPS/INS updates are corrected within several seconds using the 18 sets of tie-points. A result of horizontally registering the laser points of VLMS to the DSM is shown in Figure 8.

4.2 Applications of data fusion

An interface for semi-automatically extracting a broad range of urban objects using both laser points and line images was proposed, and an application of the interface using VLMS data was developed in our previous research (Zhao and Shibasaki 2003b). Laser points are projected onto line images. Using line images as the interface, using laser points for 3D information, manually drawing the boundary of the target objects, geometry of the objects are automatically calculated from the corresponding laser points. Figure 9 shows an example of object extraction using the interface.

On the other hand, building frames of the 1:2500 digital map can be projected onto the line images of VLMS by looking for the pixel that has the same projection vector with that of each building corner. Textures of the building facades are generated automatically by projecting and re-sampling corresponding image pixels onto the plane of the building facades. A view of the textured buildings, as well as the objects that are extracted from the VLMS data is shown in Figure 10.

5. CONCLUSION

This paper contributes to a method of fusing the data output of a mobile mapping system - VLMS with existing geographic data sources, aiming at enriching the database of urban details. An algorithm is developed to rectify the GPS/INS parameters that might be quite erroneous in urban area by registering the laser points of VLMS with an existing data source, e.g. a DSM. The algorithm is examined using a VLMS data that are taken at GINZA area, Tokyo. The laser points of VLMS are horizontally and vertically registered with a DSM, where 18 sets of tie-points are manually assigned, and four parameters at each GPS/INS update are corrected automatically and efficiently. Objects are extracted from the rectified VLMS data, which consist of commercial sign board, traffic sign/signal, road boundary, road lights etc., and fused with a 1:2500 digital map. In addition, line images of VLMS are projected onto the building facades of the digital map, and textures are generated in an automated way.

REFERENCE

[1] Collins, R., A.Hanson and E.Riseman, Site Model Acquisition under the UMass RADIUS Project, Proc. of Arpa Image Understanding Workshop, pp.351-358, November 1994.

[2] Gruen, A., 1998, TOBAGO - a semi-automated approach for the generation of 3-D building models, ISPRS Journal of Photogrammetry and Remote Sensing, vol.53, issue 2, pp.108-118.

[3] Li, R., 1997, Mobile mapping: An emerging technology for spatial data acquisition, Photogrammetric Engineering and Remote Sensing, 63(9), pp.1085-1092.

[4] El-Sheimy, N., 1999, Mobile multi-sensor systems: The new trend in mapping and GIS applications, IAG Journal of Geodesy, Vol.121, Geodesy Beyond 2000: The challenges of the first decade. Springer Verlag Berlin Heidelberg. 2000. pp.319-324.

[5] Ellum, C., N. El-Sheimy, 2000, The development of a backpack mobile mapping system, International Archives of Photogrammetry and Remote Sensing, vol.XXXII, Part B2, pp.184-191, Amsterdam.

[6] He, G., G.Orvets, 2000, Capturing road network data using mobile mapping technology, International Archives of Photogrammetry and Remote Sensing, vol.XXXIII, Part B2, pp.272-277, Amsterdam.

[7] Konno, T, et al., 2000, A New Approach to Mobile Mapping for Automated Reconstruction of Urban 3D Model,proc. of Int. Workshop on Urban Multi-Media/3D Mapping. (CD-ROM proceedings)

[8] Silva, J.F.C., P.O.Camargo, R.A.Oliveira, A street map built by a mobile mapping system, International Archives of Photogrammetry and Remote Sensing, vol.XXXIII, Part B2, pp.510-517, Amsteram.

[9] Zhao, H., R. Shibasaki, 2003a, Special Issue on Computer Vision System : Reconstructing Textured CAD Model of Urban Environment using Vehicle-borne Laser Range Scanners and Line Cameras, Machine Vision and Applications, 14 (2003) 1, 35-41.

[10] Zhao, H., R. Shibasaki, 2003b, A New Interface for Extracting Urban Spatial Objects using Vehicle-borne Laser and CCD Cameras, Proc. of Computers on Urban Planning and Urban Management, May 2003 Sendai, Japan.

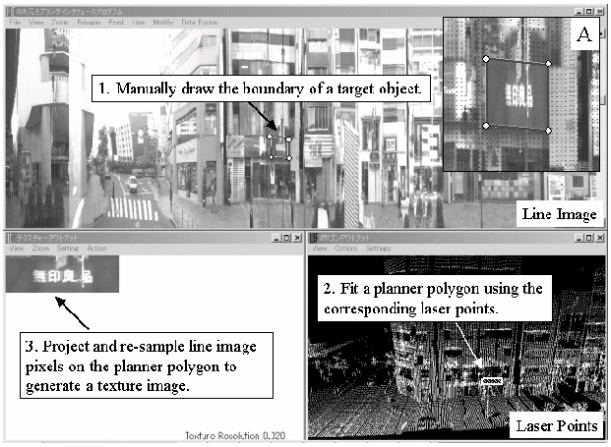

Figure 9. An example of object extraction using a semi-automated interface

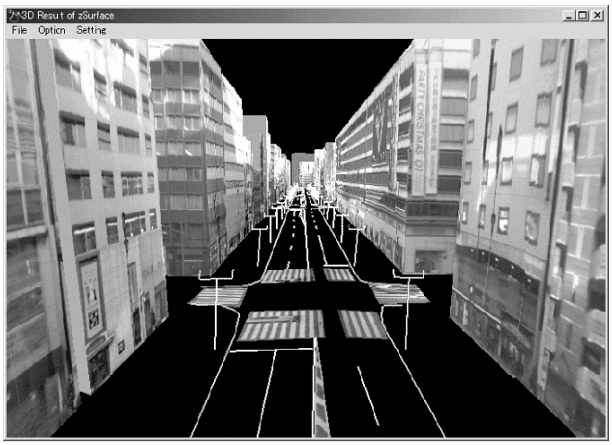

Figure 10. A view of textured building as well as the objects extracted from the VLMS data